DOLPHIN-STYLE GLIDING*

by

Richard Meyer
Akademische Fluggruppe Zurich

ABSTRACT

A quasisteady dolphin flight technique is presented for the analysis of minimum-time planar flight through an arbitrary deterministic vertical wind distribution. A piecewise-constant wind distribution is assumed. The MacCready construction for optimal thermal-to-thermal soaring is applied over each segment of constant wind intensity using a shifted velocity polar. By neglecting the sailplane dynamics, a composite "virtual polar" is constructed from these piecewise-MacCready optimal flight conditions. The usual MacCready theory can then be applied directly to this virtual polar to predict average minimum-time travel speeds, glide angles, and other performance quantities. After a discussion of the virtual polar, several performance comparisons are given for various wind distributions, wing loadings, and sailplane types.

Notation:

s = range; S = final range (normalized to one)

V_{auf} (s) = the prescribed meteorological disturbance function or vertical wind distribution (independent of altitude)

V_{st} = rise speed attained by steady circular flight within the thermal

V_h = horizontal flight speed

$V_s(V_h)$ = rate of sink in still air (actual velocity polar)

$\bar{V}_h$ = average horizontal speed attained in stationary dolphin flight

$\bar{V}_s(\bar{V}_h)$ = average rate of sink attained in stationary dolphin flight (virtual polar)

V_r = real thermal-to-thermal speed for zero altitude loss (traditional definition)

H = altitude loss during stationary dolphin flight over range S

t_{st} = rise time in circular flight required to regain altitude loss H

$t_{g\ell}$ = glide time for stationary dolphin flight over range S

1. Introduction

Numerous publications (see, for example, (1)-(4)) on dolphin soaring and countless discussions among soaring enthusiasts have had a dual effect. Although this style of soaring has been considerably clarified, there also exists some confusion because of faulty computations and erroneous inferences. At the suggestion of Rene Comte, coach of the Swiss national gliding team, a study of dolphin soaring was prepared by the Technical Division of the Academic Flight Group in Zurich. It was first presented in mid-November 1974 as part of a training course for the Swiss national gliding team. The extensions added since then and the additional results obtained thereby have encouraged the author to make the study available to a larger audience even though the excellent paper by Pirker (3) anticipates part of the results presented here.

The primary goal of this study has been to convey to the interested sailplane pilot quantitatively correct results in an easily understood and remembered fashion. To facilitate individual use and interpretation, the results are presented in the traditional way. In addition, emphasis has been placed on providing a flexible method which does not impose significant restrictions with respect to weather models or sailplane types. The only knowledge assumed of the reader is the opimality principle of stationary flight (sometimes called the MacCready Rule).

---

* A translated and edited version of "Segelflug im Delphinstil," *Aero-Revue*, Vol. 50, No. 12, 671-678, December 1975. Edited by Bjorn Pierson, Iowa State University. Reprinted by permission.

Several assumptions underlie the method developed here. The term *stationary dolphin flight* will denote that flight mode for which the speed is always the static optimal glide speed corresponding to the current vertical wind. Thus, all conditions are assumed to be quasi-stationary. That is, the flight condition can be adapted instantaneously to match the changing wind level, and the transition from one equilibrium glide condition to another occurs without dynamic losses or gains. This presupposes large-area upcurrent and downcurrent fields without abrupt transitions. Altitude is assumed to be unrestricted; flight via upcurrents and downcurrents is not impeded by cloud ceilings or by the terrain. Finally, the weather model consists of narrow upcurrent regions (thermals), in which the rise speed V_{st} is reached in steady circular flight, and of variable large-area upcurrent and downcurrent regions which are flown through dolphin-style.

2. Analysis

The optimality principle in cross-country flying (the basis for the MacCready ring and its use) is familiar to any competition sailplane pilot. In stationary dolphin flight for every setting of the ring, corresponding to V_{st}, together with the upcurrents and downcurrents encountered between thermals (V_{auf}), there results a unique optimal horizontal speed history, $V_h(s)$. At each point s , the calculation of the optimal V_h depends only on the value of V_{auf} at that point and not the entire wind distribution. The MacCready theory always yields the optimal V_h which leads to the fastest travel speed. It is easily seen that this is the case for the stated assumptions if one imagines the range divided up into small segments, each with constant upcurrent or downcurrent, which are optimized individually.

These calculations are usually made with the aid of a graph (see Fig. 1). In flying through a constant downcurrent one imagines the entire polar shifted downward by the amount of the downcurrent, and the optimality considerations are based on this shifted polar as though one had a less efficient sailplane that sinks throughout the speed range by as much more as corresponds to the strength of the downcurrent. Analogous considerations apply, of course, to the crossing of a constant upcurrent for which the polar is shifted upward by the amount of the upcurrent. One then flies with an apparently better sailplane.

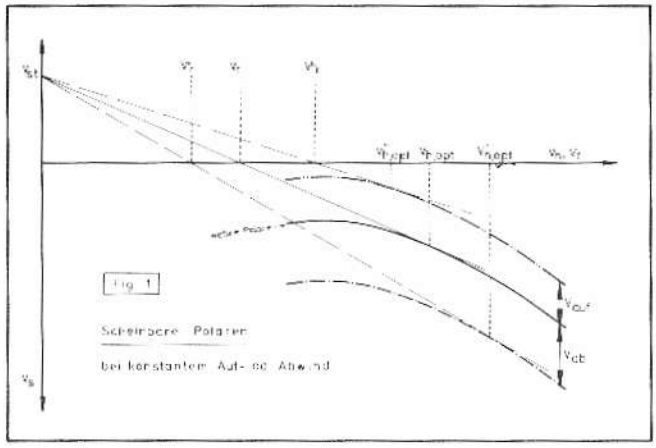

Fig. 1. Virtual polars constant upcurrent or downcurrent are obtained by a parallel shift of the true polars. The tangent construction yields, with given rise speed, the optimal horizontal and travel speeds.

Arbitrarily many upcurrents and downcurrents of arbitrary strengths and order are to be traversed in straight flight. The best travel speed is achieved if the MacCready ring is set to the maximum rise speed expected in a circular flight. This setting corresponds to the strongest expected upcurrent (thermal) minus the rate of sink (about 0.8 m/s) in circular flight. If the ring setting is not changed, the optimal flight speed will vary with range. Of course, the time needed to fly from thermal to thermal, and the altitude loss incurred in doing so, will depend on the ring setting chosen. Higher ring settings increase the speed but also increase the altitude loss. After the total gliding time and altitude loss have been determined for a given ring setting, average values for flight speed, rate of sink and glide slope can be calculated from the relations $\bar{V}_h = S/t_{g\ell}$, $\bar{V}_s = H/t_{g\ell}$, and $\bar{E} = \bar{V}_h/\bar{V}_s$, respectively.

The average speeds can now in turn be condensed into a characteristic or virtual polar in a manner similar to that for flight through uniform upcurrents or downcurrents. The virtual polar depends on the particular vertical wind distribution* used. However, the order in which the wind strengths occur is irrelevant. What does matter is merely the percentage of the total range over which each wind strength occurs. In the lower half of Fig. 2, four such virtual polars are shown. They were obtained from the true polar of a Standard Libelle at a wing loading of 28.5 kg/m^2 in conjunction with a "standard" weather

*Hereafter abbreviated by the term "wind distribution." — Ed.

model M1 which consists of 50% upcurrents and 50% downcurrents with equal strengths of 1, 2, 3 and 4 m/s.

These virtual polars can be treated just like true polars in computing average performance quantities for stationary dolphin flight. Using the usual simple tangent construction, it is possible to deduce glide angles, determine travel speeds, and carry out loss estimaes for false ring settings. The travel speed curves for the four calculated virtual polars of the Standard Libelle are also given in Fig. 2.

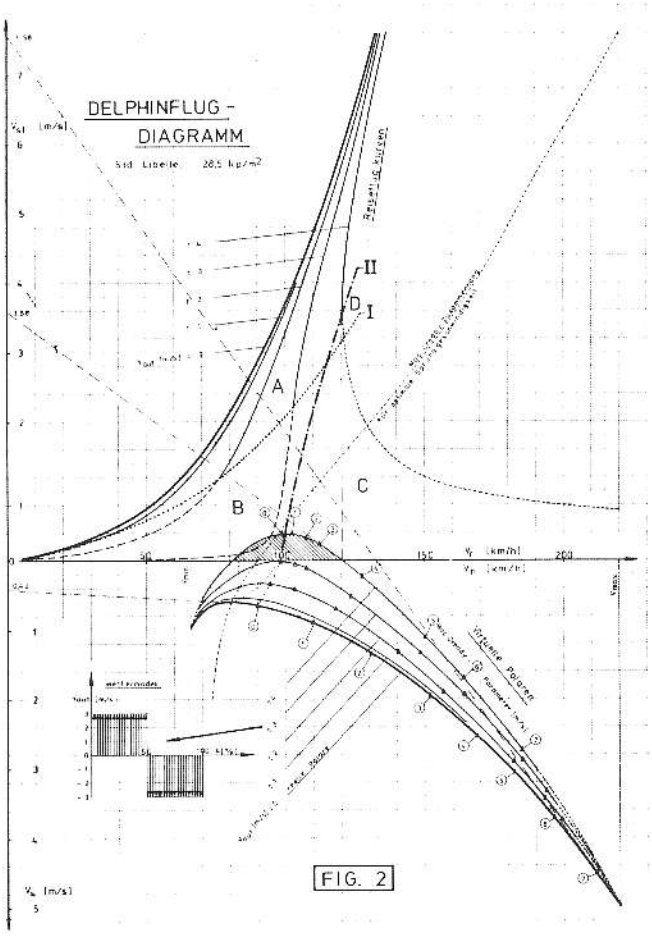

FIG. 2

Fig. 2. Complete dolphin diagram for the Standard Libelle with a wing loading of 28.5 kg/m^2 and the weather model M1.

3. The Calculation of Virtual Polars

From the true flight polar, MacCready theory and the specified vertical wind distribution, the average speed can be computed as

$$\bar{V}_h = S/t_{g\ell} = S/\{\int_0^S (1/V_h)\, ds\}. \qquad (1)$$

The average rate of sink is given by

$$\bar{V}_s = H/t_{g\ell} = \{\int_0^S [(V_s - V_{auf})/V_h]\, ds\}/\{\int_0^S (1/V_h)\, ds\}. \qquad (2)$$

Further, the travel speed can be computed as

$$V_r = S/(t_{g\ell} + t_{st}) = S/\{\int_0^S (1/V_h)\, ds + H/V_{st}\}, \qquad (3)$$

V_r can easily be obtained graphically as well.

The computation of $\bar{V}_h$, $\bar{V}_s$, and V_r proceeds best by dividing the path segment S into arbitrary subsegments over which V_{auf} can be assumed constant; that is, $V_{auf}(s)$ is approximated as a piecewise-constant function. However, this procedure is very laborious and, because of the repeatedly necessary graphical determination of V_h and associated V_s, inaccurate as well.

For this reason, a computer program has been developed to allow quick and accurate computations for arbitrary polars and weather models. The true polar is input in tabular form. Intermediate values are obtained by cubic interpolation in such a way as to guarantee a continuous tangent. Thus, even polars not easily approximated by a single parabola can be handled accurately.

Next, for a full range of ring settings, (V_h, V_s) pairs satisfying the optimality condition are computed. The corresponding travel speeds are also computed. The piecewise-constant wind distribution* is then input sequentially with both wind strength and path length given for each subsegment. The present program allows as many as 20 subsegments.

The average speeds can now be computed from Eqns. (1) and (2) for each MacCready ring setting. From these results, the virtual polar corresponding to the given wind distribution can be obtained.

---

* *Vertical* wind distribution. — Ed.

4. Discussion of a Typical Diagram

Consider again the example of a true polar and four virtual polars shown in the lower part of Fig. 2. Note that by flying through a wind distribution consisting of 50% upcurrents and 50% downcurrents (both of equal strength) the polar is improved and is, particularly in the region of the best gliding speed, strongly curved. The end points, given by the minimum and maximum speed, remain unchanged. Thus, it seems as though the sailplane became more efficient by optimal flight through upcurrent and downcurrent fields of the kind assumed except for very slow flight (strongly negative MacCready ring setting) and for very fast flight (extremely high MacCready ring setting). Moreover, the improvement increases with increasing wind amplitude. With an $|V_{auf}|$ of only 3 m/s, the virtual polar almost reaches the zero line for $\bar{V}_s$. The average glide angle becomes zero at the point of contact! Circling is no longer necessary. For $|V_{auf}| = 4$ m/s, the virtual polar exceeds the zero line for $\bar{V}_h$ in the range 81 to 120.6 km/h. Where it intersects the zero line, the altitude in dolphin flight is just maintained. Where the virtual polar lies above the zero line, altitude is gained in pure dolphin flight without circling.

The corresponding ring setting is obtained from the y-axis intercept of the virtual polar tangent. For example, with a wind strength of 4 m/s it is possible to maintain altitude by dolphin flight at a ring setting of 3.58 m/s. Specifically, upcurrents of 4 m/s will be flown through at a speed of 83.0 km/h, and downcurrents of -4 m/s will be flown through at 220 km/h (V_{max}) as dictated by the MacCready theory.

The improvement of the polars by utilizing upcurrents and downcurrents in dolphin flight strongly influences the travel speeds shown in the upper half of Fig. 2. Although the transformed polars are referred to as apparent polars, these travel speed curves are perfectly real (if one ignores the finely dashed branch). The increase in travel speed due to optimal dolphin flight is considerable.

As alluring as these results seem, it is still important to interpret them correctly. In this regard, several comments must be made. First, the results are valid only if the ring setting corresponds to the actual rate of climb while thermalling. If, for example, our sailplane exhibits an 0.8 m/s rate of sink in still air during circling flight typical of thermalling, then we will certainly encounter a V_{st} of at least $V_{st(min)} = V_{auf} - 0.8$ for the weather model selected. Thus, we will not begin thermalling unless a V_{st} greater than $V_{st(min)}$ can be attained and will set the ring at least that high. The corresponding boundary on the travel speed diagram is shown in Fig. 2 as a heavy dotted line and marked I. Points below that line will not generally be of interest since, except for isolated instances in which our altitude is dangerously low, we do not intend to begin circling for weaker upcurrents than those offered in the weather model. The properly attainable gains in travel speed are therefore limited to the area above the curve I. These gains are considerable, particularly for relatively weak upcurrents. Also, note that as V_{auf} is increased there is a corresponding decrease in the influence of V_{st} on V_r. This is because the altitude loss II, and hence the rise time t_{st} decreases with increasing V_{auf}.

Secondly, note that the special case of zero altitude loss in dolphin flight occurs at the point of intersection between the virtual polar and x-axis. The travel speed curve attains an infinite slope at that point, which means V_r is independent of V_{st}. This flight condition corresponds to a specific ring setting, which for $V_{auf} = \pm 4$ m/s can be read from Fig. 2 as 3.58 m/s. Such a ring setting can be found for every virtual polar which extends above the x-axis. The locus of these zero altitude loss points is shown in Fig. 2 by a heavy dot-dash curve marked II. To the right of this curve, climbing without circular flight is possible; to the left, altitude losses suffered in dolphin flight must be regained by thermalling.

Finally, note from Fig. 2 that the curves I and II divide the travel speed diagram into 4 regions marked A through D. Region A corresponds to mixed flight modes: partly dolphin flight and partly circling flight with only the strongest upcurrents selected for thermalling. Assuming the assumptions of Section I are met, Region A will generally be the most useful. Region B also corresponds to mixed-mode flight. However, in this case insufficient upcurrents are used for thermalling, and the ring is set back accordingly. This measure is conservative since it results in reduced travel speeds, flatter glide angles, and consequently reduced altitude losses.

Pure dolphin flight can be practiced in Regions C and D. If the terrain or the cloud base rises, or if stronger upcurrents prevail at higher altitudes so that it is advantageous to climb there, then this flight tactic may have advantages. An important comment must

be made concerning the travel speed curve in these regions (shown as a finely dashed line in Fig. 2). The reason the travel speeds seem unusually high is that if we climb in dolphin flight then, according to the definition of travel speed, a negative rise time must be inserted for the circular flight since $t_{St} = H/V_{St}$ and the altitude loss H is negative. But since this time gain is not exploitable (for example, we cannot fly over the finish line at some arbitrary altitude and then claim a time credit), these results must be regarded as impractical though mathematically correct. The small Region D corresponds to a climb in pure dolphin flight even though the ring setting is higher than V_{auf} - 0.8 m/s. Thus, it may be necessary to set the ring higher than the expected V_{St} in order to prevent one from attaining a net altitude gain during optimal dolphin flight.

5. The Effect of Variations in the Weather Model

The weather model (M1) assumed thus far, namely 50% upcurrents and 50% downcurrents of equal strength, is arbitrary and perhaps rather unrealistic. However, although *any* particular distribution is arbitrary, the consideration of additional distributions will prove useful in discovering general trends.

In weather model M2, the upcurrents will be limited to 20% of the range, and downcurrents occupy the remaining 80%. The sum of upcurrents and downcurrents will still be zero so that the upcurrents are four times as strong as the downcurrents. This model corresponds to a distribution with strong upcurrents and weak large-area downcurrents. The results for M2 are shown in Fig. 3 and reveal clearly that the attainable gains in

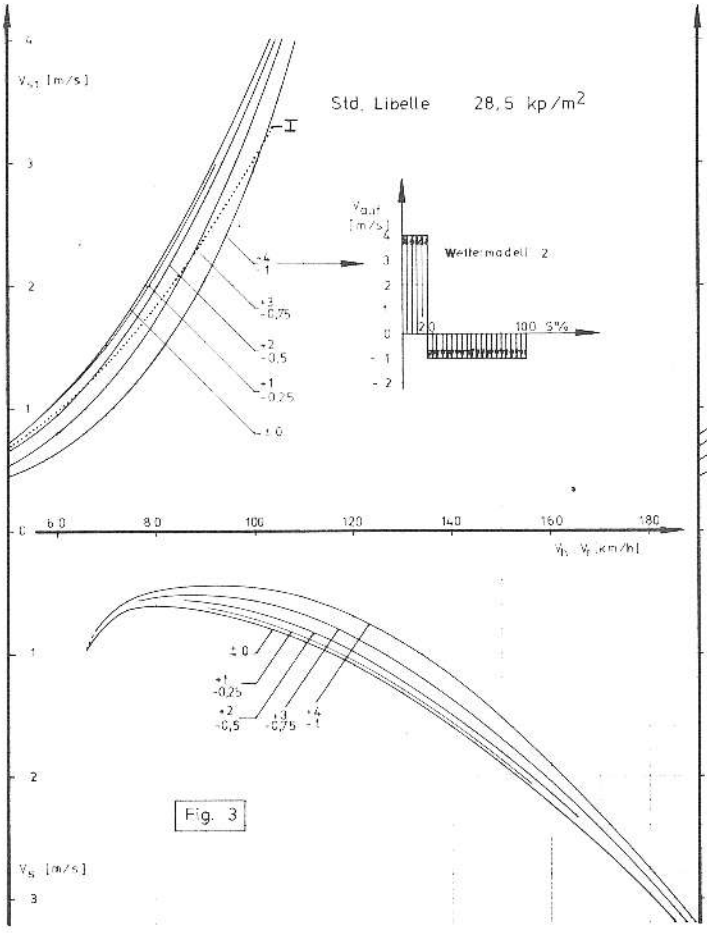

Fig. 3. Dolphin flight diagram for Standard Libelle with weather model M2: strong upcurrents and weak large-area downcurrents.

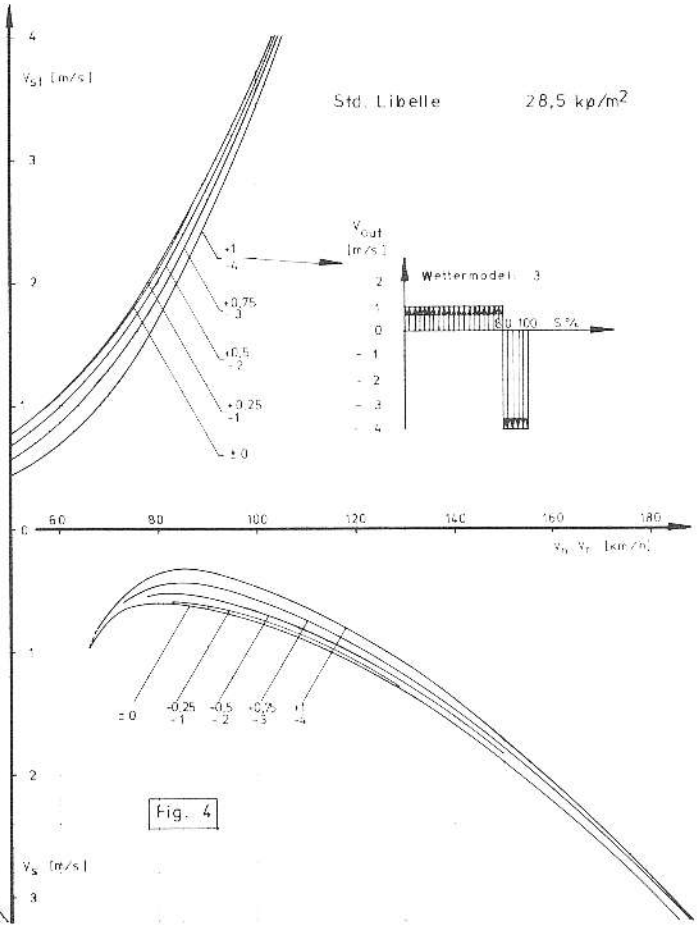

Fig. 4. Dolphin flight diagram for Standard Libelle with weather model M3: strong downcurrents and weak large-area upcurrents.

travel speed are no longer as large. The virtual polars show the greater deviations from the original polar at higher speeds when compared to the results for M1. Pure dolphin flight is not possible with M2 anywhere within the range of V_{auf} values under examination.

Weather model M3 is the mirror image of M2. Thus, M3 represents weak large-area upcurrents and strong concentrated downcurrents. The results in Fig. 4 show still more moderate effects. But it should be noted that, even with upcurrents of only 1 m/s, the travel speed has been increased by 12 km/h. The deformation of the polars is most pronounced in the region of moderate flight speeds.

M4 is a sinusoidal wind distribution with an amplitude of 4 m/s. This model has also been investigated by Kauer (2) for the Standard Cirrus. In our case, pure dolphin flight is not quite possible as can be seen in Fig. 5. If the upcurrents and downcurrents are each replaced by their average value of 2.546 m/s, model M1 results. From Fig. 5, note that M4 yields results roughly similar to those for M1 with V_{auf} between 2 and 3 m/s. Thus, the average-value approximation (M1 for M4 yields reasonably good results.

6. The Effect of Wing Loading

Consider now the weather model M1 and the Standard Libelle with a wing loading increased to 35 kg/m^2. The impressive results are shown in Fig. 6. Although the range of pure dolphin flight has become smaller (shaded region), the travel speeds have increased by yet another significant percentage. In calm air, the increase amounts to about 5 1/2%. Under in-

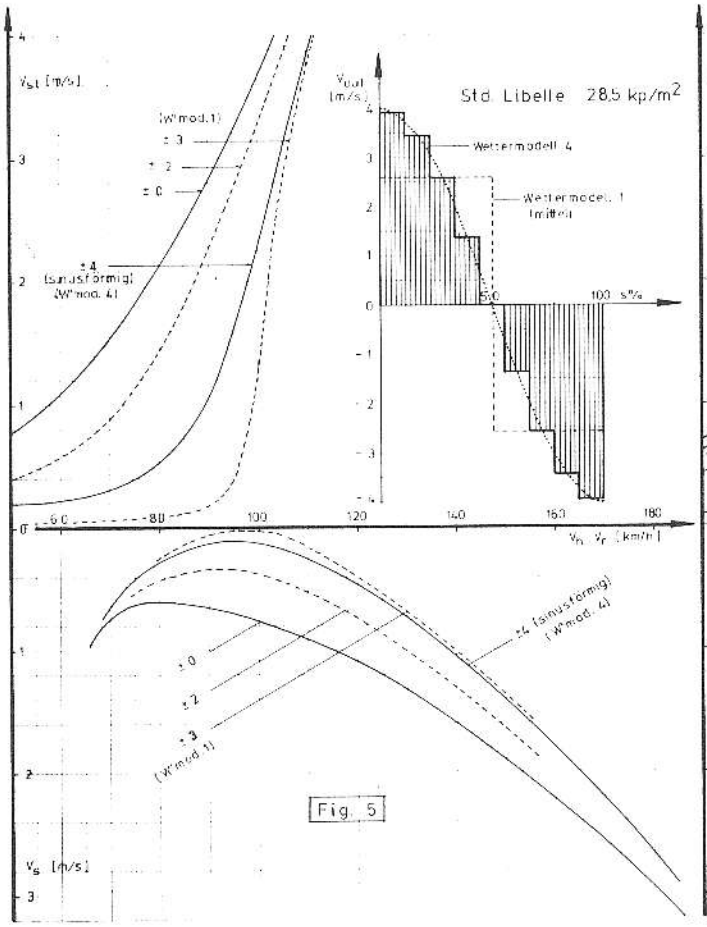

Fig. 5. Dolphin flight diagram for Standard Libelle with weather model M4: sinusoidal wind distribution with 4 m/s amplitude. For comparison purposes, the corresponding curves for weather model M1 with amplitudes of 2 and 3 m/s are also given.

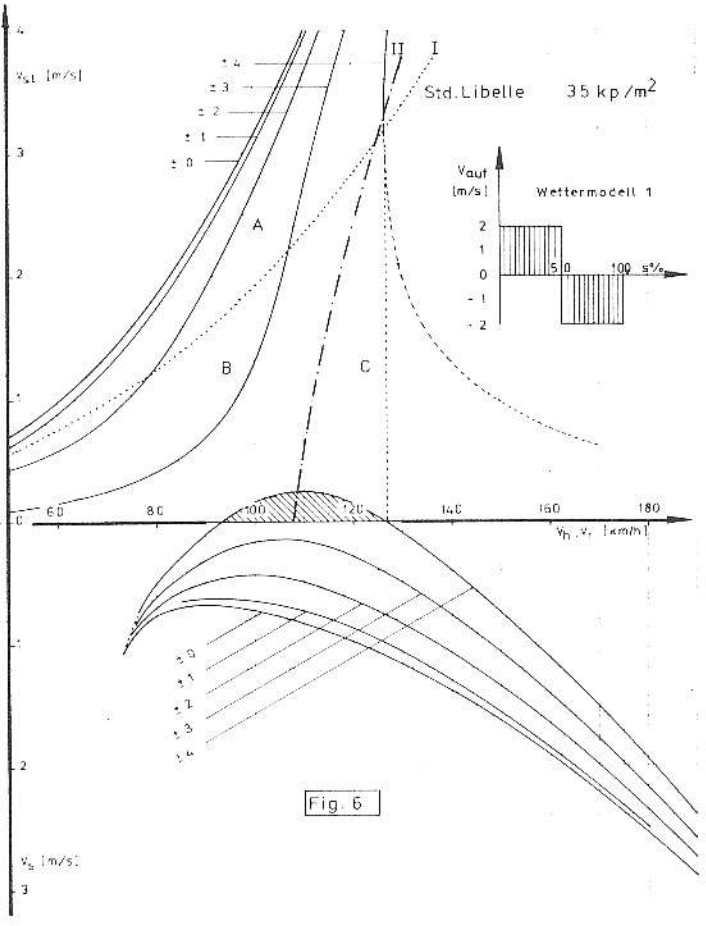

Fig. 6. Dolphin flight diagram for Standard Libelle with 35 kg/m^2 wing loading (water ballast), V_{max} = 250 km/hr and weather model M1.

creasing dolphin influence (increasing V_{auf}), the advantage shrinks somewhat for weak upcurrents of 1.5 m/s or less, but remains preserved in strong climbing. One may object that the heavier sailplane does not climb as well in upcurrents as the lighter one, and this has not been taken into account in this analysis. Basically, this is true, and in calm air the increase in travel speed is somewhat less. However, since V_r becomes increasingly insensitive to V_{st} as the boundary curve II is approached, these results are still valid. This is a further advantage of the loaded sailplane. The relevant values are shown in Table 1 for purposes of comparison.

7. The Effect of Sailplane Type

In addition to the Standard Libelle, the AS-W17 as a representative of the open class and the Ka-6CR as a representative of the club class have each been examined in conjunction with the wind distribution M1. The results are given in Figs. 7 and 8 and in Table 1. Two important conclusions emerge from this comparison. An open class sailplane, which attains a travel speed of 10 to 12 km/h more than a standard class sailplane in calm air, increases its advantage in weak thermals (V_{st} less than 2.5 m/s) as the influence of the dolphin flight mode (V_{auf}) increases. With stronger climb speeds, the advantage decreases slightly as dolphin flight influence increases. Furthermore, a standard class sailplane, which is superior to one of the club class by 10 to 20 km/h in calm air, increases its advantage in weak and medium thermals with increasing V_{auf} very substantially. For V_{st} greater than 4 m/s, however, the advantage is considerably less.

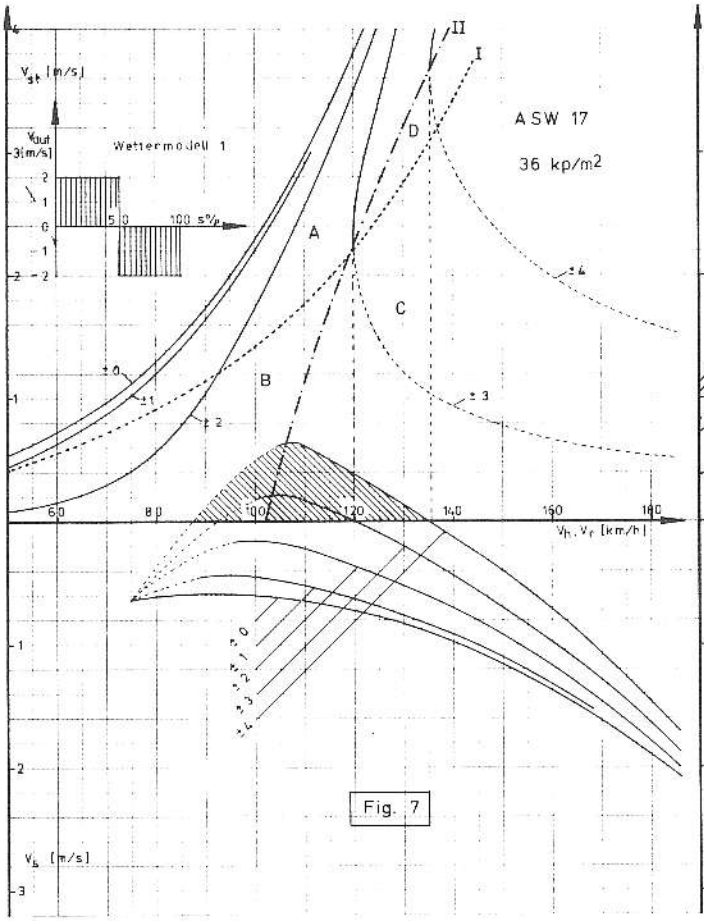

Fig. 7. Dolphin flight diagram for weather model M1 and the AS-W17: 36 kg/m^2 wing loading and operating polar.

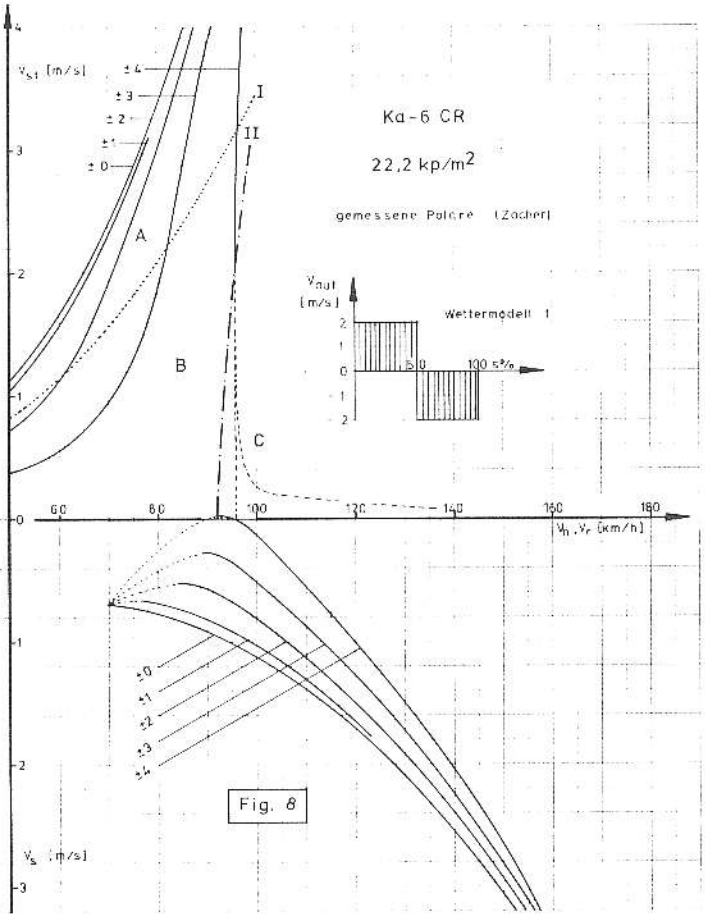

Fig. 8. Dolphin flight diagram for weather model M1 and the Ka-6CR: 22.2 kg/m^2 wing loading and polar measured by Zacher (*Aero-Revue* 10/1964).

8. The Effect of Unbalanced Weather Models

The models considered thus far contain equal volumes of upcurrents and downcurrents. In reality the pilot tries to find a path along which upcurrents dominate. Such weather models can easily be deduced from those previously examined by adding a constant amount of upcurrent everywhere. Since an additional constant upcurrent results merely in a vertical shift of the polars, it is possible to obtain without much computation the virtual polars for unbalanced weather models from the virtual polars of balanced models.

In Fig. 9 the weather model M1 with an amplitude of 2 m/s has been overlaid with various constant upcurrent strengths. The most striking fact about these results is the strong progressive increase in travel speeds even with relatively weak unbalanced upcurrent components. Although this result was to be fully expected qualitatively, the magnitude of the increases is still surprising. From this it can be concluded that, during optimum dolphin flight, very special care must be taken to fly along paths which yield as large an upcurrent surplus as possible. It is conceivable that rather substantial detours may pay off.

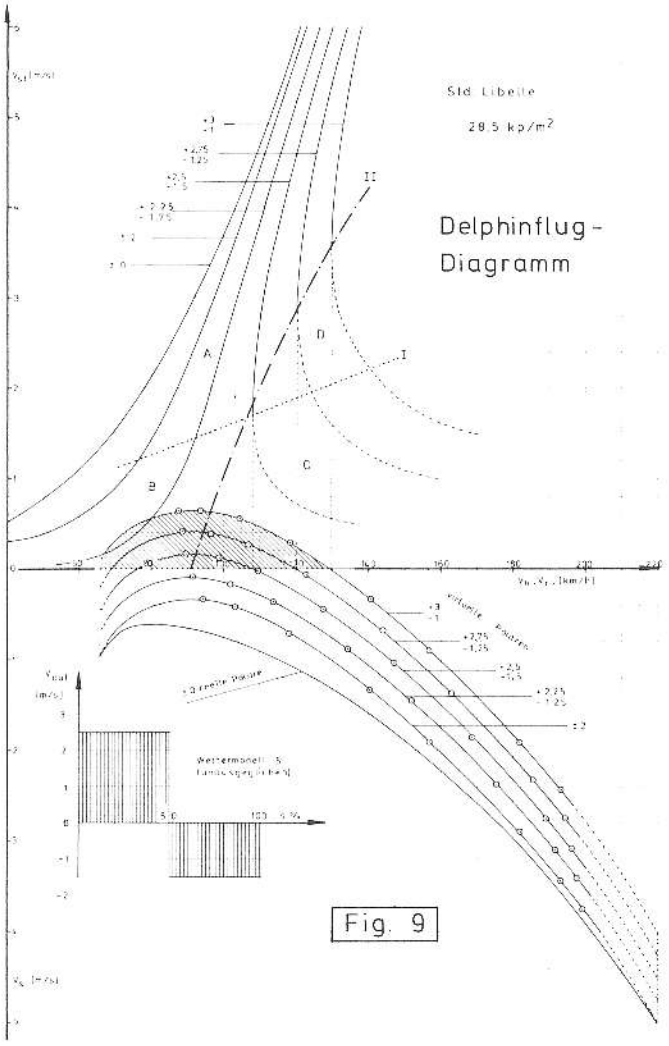

Fig. 9

Fig. 9. Dolphin flight diagram for Standard Libelle with unbalanced weather model M5: M1 with amplitude of 2 m/s overlaid with constant upcurrents of 0.25, 0.5, 0.75 and 1 m/s.

9. Summary and Concluding Remarks

The present study examines in detail and clarifies many aspects of quasi-stationary dolphin flight in relation to the usual thermalling mode of cross-country flight. The sailplane pilot is equipped with important results in a form in which they are easy to understand and use. The mode of presentation chosen here is particularly useful since one can manipulate the apparent polars exactly the same as true ones. Although any weather model is unrealistic in the sense that it will never occur in exactly the assumed form in nature, it is felt that there are typical weather situations which can be better exploited through a deeper understanding of dolphin flight and a knowledge of the most important rules elaborated here. Finally, it should be noted that the method of computation developed here is quite general in that practically any weather model and any sailplane polar can be accepted as input data.

REFERENCES

1. Favarger, D.: "Vitesse de croisiere d'un planeur, utilisant des rues de nuages," *Aero-Revue*, Dec. 1968, Jan. 1969.

2. Kauer, E. and Junginger, H.G.: "Segelflug in Delphinstil," *Aero-Kurier*, Sept. 1973, Oct. 1973.

3. Pirker, H.: "Uber die Reisegeschwindigkeit von Segelflugzeugen, 2. Teil: Der Delphinflug," *Flugsportzeitung*, Jan. 1975.

4. Bohli, H.: "Optimale Delphinfluggeschwindigkeit auf Streckenflugen," *Aero-Revue*, Aug. 1971.

Table 1. Comparison of maximum travel speeds of different sailplanes for weather model M1.

V_{st}	V_{auf}	Ka-6CR 22.2 kg/m^2 (wing loading)	Std. Lib. 28.5 kg/m^2	Std. Lib. 35 kg/m^2	AS-W17 36 kg/m^2
1	0	47.12	57.65	60.74	71.17
	±1	49.47	60.80	63.71	74.35
	±2	57.48	72.75	74.12	89.52
2	0	64.94	78.08	82.94	94.97
	±1	66.33	80.14	84.85	97.06
	±2	71.00	87.26	91.83	103.58
	±3	80.92	102.24	105.87	119.9*
3	0	76.76	92.11	97.79	110.45
	±1	77.41	93.49	99.35	111.45
	±2	80.06	97.49	103.56	115.06
	±3	85.74	105.69	111.89	122.34
	±4	96.16	120.5*	126.0*	136.5*
4	0	85.64	103.73	110.26	122.04
	±1	86.21	104.21	110.87	122.59
	±2	87.78	106.51	113.54	124.50
	±3	91.01	111.54	118.54	128.70
	±4	97.13	120.75	127.30	136.37
5	0	93.08	113.12	120.55	131.25
	±1	93.41	113.57	121.03	131.62
	±2	94.55	115.01	122.40	132.85
	±3	96.59	118.21	125.50	135.36
	±4	100.24	123.66	130.81	140.04

*Pure dolphin flight.